ISSN 2413-6212 (Online), ISSN 2227-1252 (Print)
Bridges and tunnels: theory, research, practice, 2026, № 29

BRIDGES AND TUNNELS: THEORY, RESEARCH, PRACTICE

UDC 624.131.5:693.972

I. M. BAKAN

SBK Group LLC, 3551 Seaward cir, apt. 342, Oceanside CA, USA, 92056,
tel. +38 (067) 436 91 21, e-mail sbc.group.ua@gmail.com, ORCID 0009-0008-4279-9793

EVALUATION OF LATERAL SOIL PRESSURE FOR MONOLITHIC COLUMN FOUNDATION OF INDUSTRIAL BUILDINGS

Purpose. The main objective of this publication is to quantitatively evaluate the effect of lateral soil pressure on the reinforcement design of the foundation system for a frame-type industrial building. **Methodology.** To achieve the set goal, the performance of the load-bearing frame model for a two-span industrial building at the casting and rolling complex of Uzmetkombinat JSC (in the city of Bekabad, Tashkent Region, Uzbekistan) was analyzed. The building overall dimensions are 129×65.25 m with a maximum height of 43.56 m. The foundation system is of the isolated type with a separate truss frame and is constructed of monolithic reinforced concrete. The modelling was carried out using the LIRA-CAD design and calculation package with the additional GRUNT module. The modelling took into account actual ground conditions. Not only traditional static loads but also seismic effects of magnitude 8.0 on the Richter scale were considered. **Findings.** A quantitative comparison of the magnitudes and distribution characteristics of the stress-strain state of the foundation system showed that taking into account the lateral pressure of the backfill soil allows the required reinforcement to be reduced by up to two times. This results in a more uniform distribution of forces within the foundation system, which is particularly important in cases where individual foundations have different embedment depths. **Originality.** The analysis quantitatively determined the extent of the influence of lateral pressure from the backfill soil on the foundation system. The necessity of its correct modelling has been demonstrated, as this significantly influences the stress-strain state of the foundation system as a whole. **Practical value.** The results obtained from the quantitative evaluation of the effect of lateral pressure on the performance of the monolithic column foundation not only enable a more informed design of the reinforcement scheme for the foundation system, but also open up prospects for incorporating this approach into Ukraine's regulatory framework.

Keywords: foundation system; isolated footing; steel frame; bedding coefficient; finite element method; LIRA-CAD complex

Introduction

Column (isolated) foundations are a classic structural element used in many types of building structures. As is well known, their main function is to transfer loads from the above-ground parts of the structure to the footing. In doing so, the nature of the load distribution must ensure the bearing capacity of the footing in accordance with the requirements of the limit state design (DBN V.2.1-10:2018, 2018).

A typical structural solution for such foundations in engineering practice involves constructing them as a vertical section (column footing) and a horizontal distribution section (bedding) (Figure 1). In international practice, the bedding is usually designed as a solid single-stage mass. In domestic practice, the bedding is designed to consist of several steps, each subsequent one having a smaller plan dimension than the previous one. This design solution allows for some material savings, provided the footing base dimensions are correctly determined. Generally, such column foundations are used for columns in the structural layouts of frame-type buildings. However, their scope of application is quite broad – ranging from supports for ordinary advertising hoardings to complex engineering structures.

The behavior of such foundations under load has now been studied quite thoroughly. Numerous studies on this topic are available, both by domestic and foreign authors. However, a significant proportion of such research focuses on evaluating the analytical model of the "foundation"-"soil mass" system for complex-type foundations (Dubinchyk, Bannikov, Kildieiev, & Kharchenko, 2020; Petrenko, Bannikov, Kharchenko, & Tkach, 2022). Another distinct area of research is the

DOI: https://doi.org/10.15802/bttrp2026-29-02

analysis of soil mass behavior for underground and above-ground construction (Alkhdour, Tiutkin, Bannikov, & Heletiuk, 2023; Bannikov, Tiutkin, 2020).

Figure 1. Monolithic column foundation

The extremely widespread adoption in engineering practice of the modern numerical method of structural mechanics – the finite element method (Bofang, 2018; Chen & Yang, 2020) – allows for a fresh re-examination of certain aspects of the "foundation – soil mass" system. In this context, the importance of correct evaluation of the footing resistance is emphasized. A prerequisite for this is the creation of accurate computational models of the footing that take into account its multi-layered nature and the variability of the properties of each layer within the soil thickness. Such approaches are of particular importance for complex building structures that are of considerable size and are subjected to high-intensity loads, including dynamic ones.

Purpose

In view of the above, the main purpose of the study is to evaluate the performance of an isolated foundation for a highly complex building structure, taking into account the multi-layered nature of the soil and dynamic loads.

Methodology

To achieve this purpose, Production Building No. 4 of the continuous steel casting department (Figure 2, *a*) was selected as the subject of the study; this building forms part of the casting and rolling complex of Uzmetkombinat JSC (Figure 2, *b*). The complex is located in the district of Bekabad city of the Tashkent region (Uzbekistan).

The building in question has two spans: one measuring 35.75 m with a total length of 129 m, and the other measuring 29.5 m with a total length of 60 m. The height of the first span to the underside of the trusses is 33.9 m, whilst the total height, including the roof skylights, is 43.56 m. The height of the second span to the bottom of the trusses is 17.6 m (along the side row of columns) and 20.45 m (along the central row of columns), with a total height of 20.3 m and 23.6 m, respectively.

The building is constructed using a steel frame structure. The column spacing varies between 12 and 24 m and is designed to be irregular along the length of the building. The steel trusses have an external trapezoidal outline and an internal triangular lattice with additional struts. To withstand the loads from the weight of the external wall cladding and horizontal wind pressure, a steel truss frame on separate foundations is provided.

The foundations are constructed from monolithic reinforced concrete with steel reinforcement. The depth of the main frame foundations varies from 6.0 m to 11.5 m. The increase in foundation depth is achieved by increasing the height of the column footing. The height of the foundation bedding remains unchanged at 900 mm. In total, the project envisaged 26 types of foundations for the main frame. The foundations of the truss frame are located at a uniform depth of 2.4 m.

To assess the performance of the building foundation system, a numerical method of structural mechanics was used – the finite element method. All calculations were performed using the LIRA-CAD 2024 design and calculation package (Barabash, Soroka, Surianinov, 2018; LIRA-CAD, 2022), using the official licensed version of the product R 2.3×64.

The computational model constructed is shown in Figure 3. The main load-bearing elements of the building steel frame structure are modeled using bar finite elements. Monolithic foundations were modeled using a combined approach – bar finite elements were used for the column footing, whilst the bedding was modeled using plate finite elements. The bedding steps were modeled using the "rigid inserts" function, which allows the central planes of the plates to be offset relative to one another (Figure 4). The total volume of the computational model comprised 31,025 finite elements and 18,478 nodes.

DOI: https://doi.org/10.15802/bttrp2026-29-02

ISSN 2413-6212 (Online), ISSN 2227-1252 (Print)
Bridges and tunnels: theory, research, practice, 2026, № 29

a)

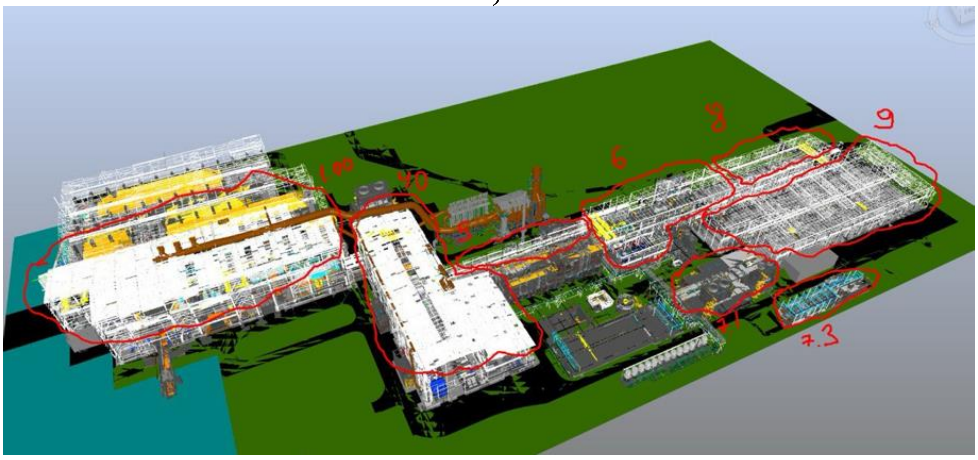

b)

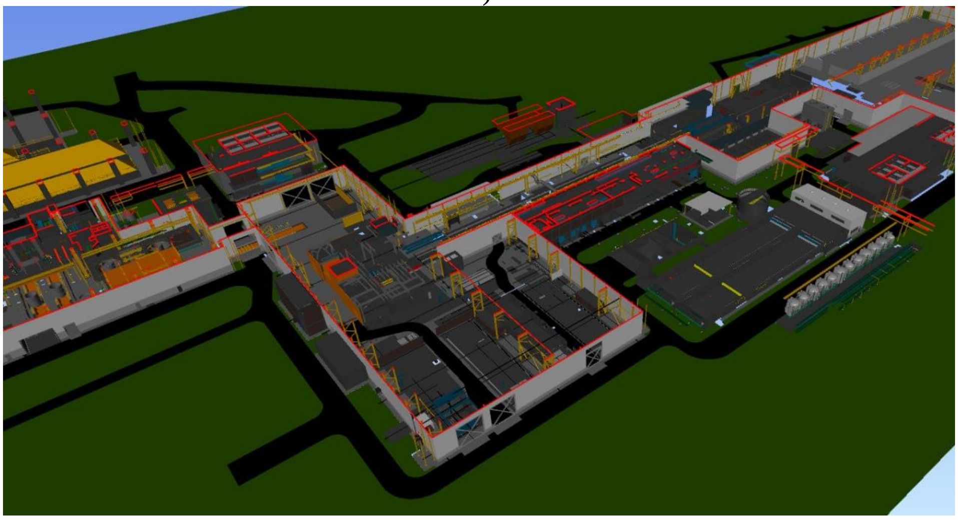

Figure 2. 3D model of the casting and rolling complex of Uzmetkombinat JSC:
a) general view with building numbers; *b*) internal structure

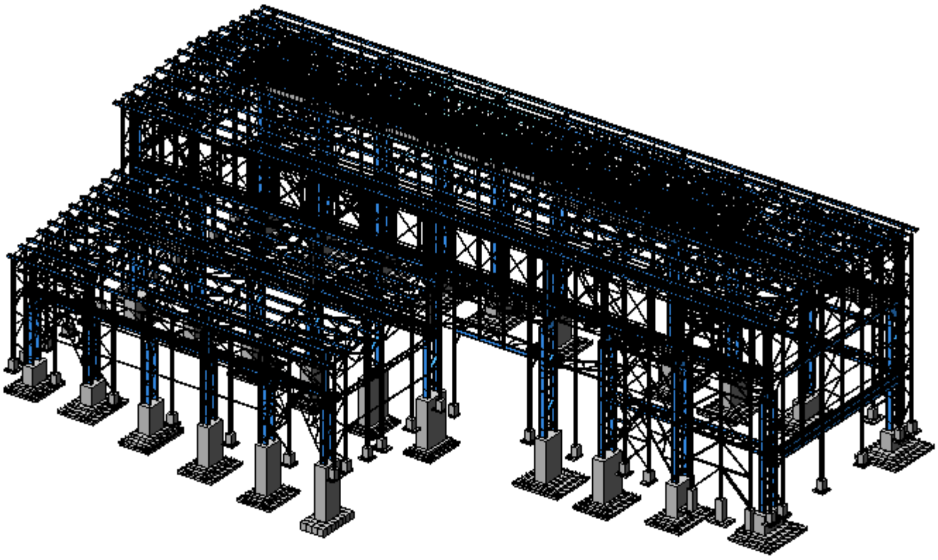

Figure 3. Computational model of building No. 4 of the continuous steel casting department

DOI: https://doi.org/10.15802/bttrp2026-29-02

The ground conditions at the site of building No. 4 are represented by two engineering-geological elements (EGE) – coarse-grained gravelly and crushed stone soils. Based on the data from the engineering-geological survey, a system of boreholes with depths ranging from 15.0 to 42.0 m was modeled in the GRUNT software module (Figure 5). On this basis, a soil model was created (Figure 6) with the relevant characteristics assigned to each EGE.

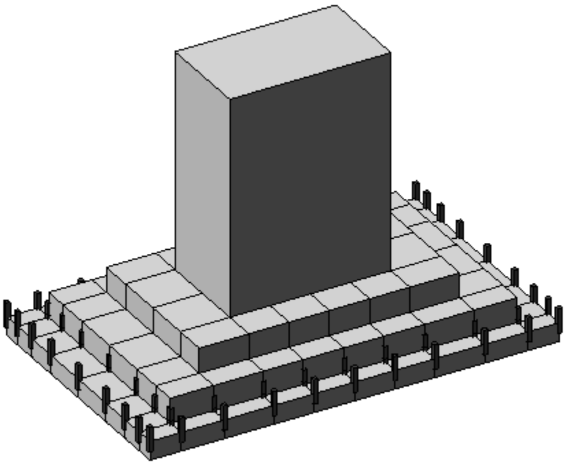

Figure 4. Computational model of the main frame foundation

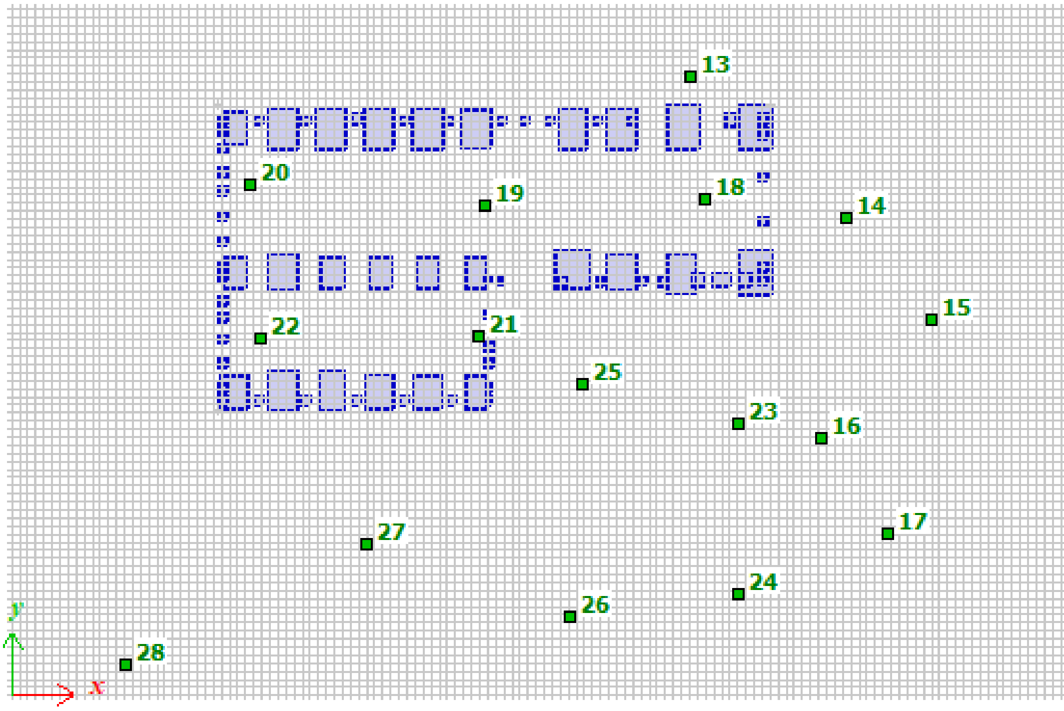

Figure 5. Model of boreholes for building No. 4

The loads specified included the dead load of structures and finishing elements, operational load, snow and wind loads together with wind pulsations, as well as crane loads in accordance with the requirements of the current standard KMK 2.01.07-96 (KMK 2.01.07-96, 1996). Also, in accordance with the requirements of standard KMK 2.01.03-19 (KMK 2.01.03-19, 2019), seismic loads were modeled – 8.0 points for the construction site. Soil category according to seismic properties is II.

It should be noted that, as a first approximation, the effect of the soil on the foundation structure was taken into account solely through the vertical pressure exerted on the horizontal steps of the

DOI: https://doi.org/10.15802/bttrp2026-29-02

ISSN 2413-6212 (Online), ISSN 2227-1252 (Print)
Bridges and tunnels: theory, research, practice, 2026, № 29

foundation bedding. The density of the backfill soil was assumed to be 1800 kg/m³.

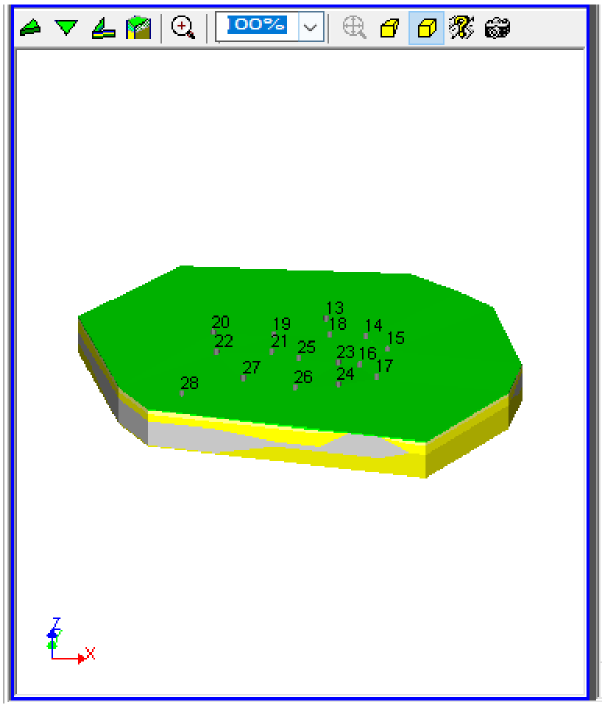

Figure 6. Model of the soil mass

Findings

During the calculations of the constructed building model, it was found that the problem is geometrically non-linear – the stress-strain state (SSS) of the soil foundation depends on the SSS of the structure itself; however, the distribution of forces in the soil foundation will in turn affect the distribution of forces in the structure. Therefore, to obtain a correct result, the calculation process must be iterative – the values of soil foundation resistance obtained in the previous step are applied to the footing base, and in the next step the stress-strain state is adjusted. As practical calculations showed, this problem required approximately 10 such iterative steps, after which the results stabilized.

A comparison of the final results with the design specifications revealed that, for some foundations, the calculated reinforcement values exceed those specified in the design (highlighted in color in Table 1). These are foundations Fm-2 – Fm-5; Fm-10 – Fm-14 and Fm-17 – Fm-21, which have the greatest embedment depth – approximately 8–11 m. Therefore, an analysis of the overall behavior of the frame structure revealed that, when subjected to horizontal seismic loads, these foundations bear the main forces. In terms of their design scheme, their behavior resembles a cantilever system. This results in the buckling of the column footing, which requires increased reinforcement. If the depth of these foundations is reduced, the situation evens out and other foundations, which were previously involved to a much lesser extent, begin to contribute to the load-bearing.

Such a redistribution of forces was most likely not taken into account during the design work, as it requires a “manual” analysis of a system that is statically indeterminate in many instances, and is in essence a rather laborious and complex task. However, this particular feature of the building frame behavior was identified during numerical calculations.

To bring the foundation behavior closer to the actual operating conditions, the task of calculating the backfill soil pressure on the lateral surfaces of the footing was implemented. To this end, the option to determine the bedding coefficients in the horizontal direction was selected. The calculations were performed automatically. As in the previous case, an iterative calculation process was implemented. The resulting reinforcement values are shown in Table 1.

Table 1

Results of the reinforcement design for the main frame foundation

Brand	Reinforcement type	Reinforcement required according to		
		design	calculation witout a lateral coeficient	calculation with a lateral coefficient
Fm-1	FF – longitudinal, cm²	443.02	197.72	67.36
	FF – transverse, cm²	10Ø8*200	2Ø4*200	2Ø4*200
	B – along the X-axis, Ø*pitch (mm)	Ø25*200	Ø25*200	Ø14*200
	B – along the Y-axis, Ø*pitch (mm)	Ø25*200	Ø18*200	Ø14*200
Fm-2	FF – longitudinal, cm²	418.40	360.81	127.39
	FF – transverse, Ø*pitch (mm)	9Ø8*200	2Ø4*200	2Ø4*200
	B – along the X-axis, Ø*pitch (mm)	Ø25*200	Ø32*200	Ø18*200
	B – along the Y-axis, Ø*pitch (mm)	Ø25*200	Ø28*200	Ø22*200

DOI: https://doi.org/10.15802/bttrp2026-29-02

ISSN 2413-6212 (Online), ISSN 2227-1252 (Print)
Bridges and tunnels: theory, research, practice, 2026, № 29

Brand	Reinforcement type	Reinforcement required according to		
		design	calculation witout a lateral coeficient	calculation with a lateral coefficient
Fm-3	FF – longitudinal, cm²	443.02	138.46	67.36
	FF – transverse, Ø*pitch (mm)	10Ø8*200	2Ø4*200	2Ø4*200
	B – along the X-axis, Ø*pitch (mm)	Ø25*200	Ø18*200	Ø14*200
	B – along the Y-axis, Ø*pitch (mm)	Ø25*200	Ø18*200	Ø14*200
Fm-4	FF – longitudinal, cm²	443.02	943.04	325.44
	FF – transverse, Ø*pitch (mm)	10Ø8*200	2Ø8*200	2Ø4*200
	B – along the X-axis, Ø*pitch (mm)	Ø25*200	Ø32*200	Ø20*200
	B – along the Y-axis, Ø*pitch (mm)	Ø25*200	Ø32*200	Ø22*200
Fm-5	FF – longitudinal, cm²	443.02	870.84	442.97
	FF – transverse, Ø*pitch (mm)	10Ø8*200	2Ø8*200	2Ø4*200
	B – along the X-axis, Ø*pitch (mm)	Ø25*200	Ø32*200	Ø22*200
	B – along the Y-axis, Ø*pitch (mm)	Ø25*200	Ø32*200	Ø25*200
Fm-6	FF – longitudinal, cm²	430.71	122.86	88.52
	FF – transverse, Ø*pitch (mm)	9Ø8*200	2Ø4*200	2Ø4*200
	B – along the X-axis, Ø*pitch (mm)	Ø25*200	Ø20*200	Ø14*200
	B – along the Y-axis, Ø*pitch (mm)	Ø25*200	Ø16*200	Ø14*200
Fm-7	FF – longitudinal, cm²	430.71	100.03	65.98
	FF – transverse, Ø*pitch (mm)	9Ø8*200	2Ø4*200	2Ø4*200
	B – along the X-axis, Ø*pitch (mm)	Ø25*200	Ø20*200	Ø14*200
	B – along the Y-axis, Ø*pitch (mm)	Ø25*200	Ø18*200	Ø14*200
Fm-8	FF – longitudinal, cm²	566.08	371.95	201.23
	FF – transverse, Ø*pitch (mm)	9Ø8*200	2Ø10*200	2Ø4*200
	B – along the X-axis, Ø*pitch (mm)	Ø25*200	Ø20*200	Ø14*200
	B – along the Y-axis, Ø*pitch (mm)	Ø25*200	Ø22*200	Ø18*200
Fm-9	FF – longitudinal, cm²	430.71	319.59	189.96
	FF – transverse, Ø*pitch (mm)	10Ø8*200	2Ø6*200	2Ø4*200
	B – along the X-axis, Ø*pitch (mm)	Ø25*200	Ø16*200	Ø12*200
	B – along the Y-axis, Ø*pitch (mm)	Ø25*200	Ø20*200	Ø16*200
Fm-10	FF – longitudinal, cm²	443.02	490.01	196.40
	FF – transverse, Ø*pitch (mm)	10Ø8*200	2Ø5*200	2Ø4*200
	B – along the X-axis, Ø*pitch (mm)	Ø25*200	Ø32*200	Ø18*200
	B – along the Y-axis, Ø*pitch (mm)	Ø25*200	Ø25*200	Ø22*200
Fm-11	FF – longitudinal, cm²	516.85	355.53	114.98
	FF – transverse, Ø*pitch (mm)	7Ø8*200	2Ø4*200	2Ø4*200
	B – along the X-axis, Ø*pitch (mm)	Ø28*100	Ø25*200	Ø14*200
	B – along the Y-axis, Ø*pitch (mm)	Ø25*200	Ø18*200	Ø14*200
Fm-12	FF – longitudinal, cm²	381.49	318.33	96.58
	FF – transverse, Ø*pitch (mm)	7Ø8*200	2Ø5*200	2Ø4*200
	B – along the X-axis, Ø*pitch (mm)	Ø25*200	Ø28*200	Ø16*200
	B – along the Y-axis, Ø*pitch (mm)	Ø25*200	Ø25*200	Ø14*200
Fm-13	FF – longitudinal, cm²	369.18	274.36	50.12
	FF – transverse, Ø*pitch (mm)	6Ø8*200	2Ø4*200	2Ø4*200
	B – along the X-axis, Ø*pitch (mm)	Ø25*200	Ø25*200	Ø16*200
	B – along the Y-axis, Ø*pitch (mm)	Ø25*200	Ø20*200	Ø14*200
Fm-14	FF – longitudinal, cm²	369.18	212.82	50.12
	FF – transverse, Ø*pitch (mm)	6Ø8*200	2Ø4*200	2Ø4*200
	B – along the X-axis, Ø*pitch (mm)	Ø20*200	Ø22*200	Ø16*200
	B – along the Y-axis, Ø*pitch (mm)	Ø20*200	Ø16*200	Ø16*200
Fm-15	FF – longitudinal, cm²	369.18	185.93	77.03
	FF – transverse, Ø*pitch (mm)	6Ø8*200	2Ø12*200	2Ø4*200
	B – along the X-axis, Ø*pitch (mm)	Ø28*200	Ø22*200	Ø16*200
	B – along the Y-axis, Ø*pitch (mm)	Ø28*200	Ø18*200	Ø14*200
Fm-16	FF – longitudinal, cm²	369.18	149.37	77.02
	FF – transverse, Ø*pitch (mm)	6Ø8*200	2Ø4*200	2Ø4*200
	B – along the X-axis, Ø*pitch (mm)	Ø25*200	Ø22*200	Ø14*200
	B – along the Y-axis, Ø*pitch (mm)	Ø25*200	Ø18*200	Ø14*200

DOI: https://doi.org/10.15802/bttrp2026-29-02

ISSN 2413-6212 (Online), ISSN 2227-1252 (Print)
Bridges and tunnels: theory, research, practice, 2026, № 29

Brand	Reinforcement type	Reinforcement required according to		
		design	calculation witout a lateral coeficient	calculation with a lateral coefficient
Fm-17	FF – longitudinal, cm²	553.77	480.21	159.18
	FF – transverse, Ø*pitch (mm)	8Ø8*200	2Ø8*200	2Ø4*200
	B – along the X-axis, Ø*pitch (mm)	Ø25*100	Ø32*200	Ø20*200
	B – along the Y-axis, Ø*pitch (mm)	Ø25*200	Ø22*200	Ø20*200
Fm-18	FF – longitudinal, cm²	418.40	308.11	74.49
	FF – transverse, Ø*pitch (mm)	8Ø8*200	2Ø4*200	2Ø4*200
	B – along the X-axis, Ø*pitch (mm)	Ø28*200	Ø28*200	Ø16*200
	B – along the Y-axis, Ø*pitch (mm)	Ø28*200	Ø20*200	Ø16*200
Fm-19	FF – longitudinal, cm²	418.40	596.39	402.49
	FF – transverse, Ø*pitch (mm)	8Ø8*200	2Ø10*200	2Ø4*200
	B – along the X-axis, Ø*pitch (mm)	Ø25*200	Ø32*200	Ø22*200
	B – along the Y-axis, Ø*pitch (mm)	Ø25*200	Ø28*200	Ø25*200
Fm-20	FF – longitudinal, cm²	418.40	560.17	391.93
	FF – transverse, Ø*pitch (mm)	8Ø8*200	2Ø10*200	2Ø4*200
	B – along the X-axis, Ø*pitch (mm)	Ø25*200	Ø28*200	Ø22*200
	B – along the Y-axis, Ø*pitch (mm)	Ø25*200	Ø25*200	Ø22*200
Fm-21	FF – longitudinal, cm²	418.40	266.05	74.49
	FF – transverse, Ø*pitch (mm)	8Ø8*200	2Ø4*200	2Ø4*200
	B – along the X-axis, Ø*pitch (mm)	Ø25*200	Ø28*200	Ø18*200
	B – along the Y-axis, Ø*pitch (mm)	Ø25*200	Ø22*200	Ø16*200
Fm-22	FF – longitudinal, cm²	418.40	191.45	63.91
	FF – transverse, Ø*pitch (mm)	8Ø8*200	2Ø4*200	2Ø4*200
	B – along the X-axis, Ø*pitch (mm)	Ø25*200	Ø22*200	Ø16*200
	B – along the Y-axis, Ø*pitch (mm)	Ø25*200	Ø16*200	Ø14*200
Fm-23	FF – longitudinal, cm²	418.40	169.98	85.07
	FF – transverse, Ø*pitch (mm)	8Ø8*200	2Ø4*200	2Ø4*200
	B – along the X-axis, Ø*pitch (mm)	Ø25*200	Ø25*200	Ø18*200
	B – along the Y-axis, Ø*pitch (mm)	Ø25*200	Ø16*200	Ø14*200
Fm-24	FF – longitudinal, cm²	418.40	275.84	212.05
	FF – transverse, Ø*pitch (mm)	8Ø8*200	2Ø8*200	2Ø4*200
	B – along the X-axis, Ø*pitch (mm)	Ø28*200	Ø25*200	Ø18*200
	B – along the Y-axis, Ø*pitch (mm)	Ø28*200	Ø20*200	Ø20*200
Fm-25	FF – longitudinal, cm²	418.40	238.56	169.72
	FF – transverse, Ø*pitch (mm)	8Ø8*200	2Ø8*200	2Ø4*200
	B – along the X-axis, Ø*pitch (mm)	Ø25*200	Ø22*200	Ø16*200
	B – along the Y-axis, Ø*pitch (mm)	Ø25*200	Ø20*200	Ø18*200
Fm-26	FF – longitudinal, cm²	418.40	190.42	159.13
	FF – transverse, Ø*pitch (mm)	8Ø8*200	2Ø8*200	2Ø4*200
	B – along the X-axis, Ø*pitch (mm)	Ø20*200	Ø16*200	Ø14*200
	B – along the Y-axis, Ø*pitch (mm)	Ø20*200	Ø16*200	Ø14*200

Note: FF – foundation footing; B – footing base

As can be seen, the required reinforcement turned out to be significantly lower than when the lateral coefficient was not taken into account. This indicates the need to adjust the calculation results when designing isolated foundations by accounting for the lateral pressure of the soil mass. At the same time, for all foundations, the reinforcement does not exceed the values adopted in the design.

From the point of view of design methodology, it should be noted that although current standards do not provide for the possibility of accounting for the lateral coefficient for column foundations, such calculations are nevertheless necessary in engineering practice.

Regarding the performance of other necessary checks in accordance with the Uzbekistan standard KMK 2.02.01-98 (KMK 2.02.01-98, 1998), the following should be noted.

Figure 7 shows the distribution of vertical reactions from the ground foundation to the footing base of the foundation system. The FM-1 foundation is subject to the highest load. The maximum pressure beneath its base is 51.1 t/m² (average pressure 43.4 t/m²), which is lower than the design

DOI: https://doi.org/10.15802/bttrp2026-29-02

ISSN 2413-6212 (Online), ISSN 2227-1252 (Print)
Bridges and tunnels: theory, research, practice, 2026, № 29

soil resistance R_0 = 60.0 t/m² for the bearing layers EGE-1 and EGE-2 according to engineering-geological survey data.

Figure 8 shows the distribution of foundation settlement of the main frame of the building under consideration. As can be seen, the settlement is highly non-uniform, which highlights its statically indeterminate behavior under load. The obtained values were analyzed for design load combinations of the main type and special type. The maximum settlement is -29.3 mm, which is below the permissible limit of 120 mm in accordance with Appendix 4 of KMK 2.02.01-98 (KMK 2.02.01-98, 1998). The maximum relative difference in settlement was: in the longitudinal direction (29.3 – 9.3) / 84,110 = 0.00024; in the transverse direction (28.5 – 7.7) / 65,425 = 0.00027. For both directions, the values obtained are less than the permissible value of 0.004 in accordance with Appendix 4 of KMK 2.02.01-98 (KMK 2.02.01-98, 1998).

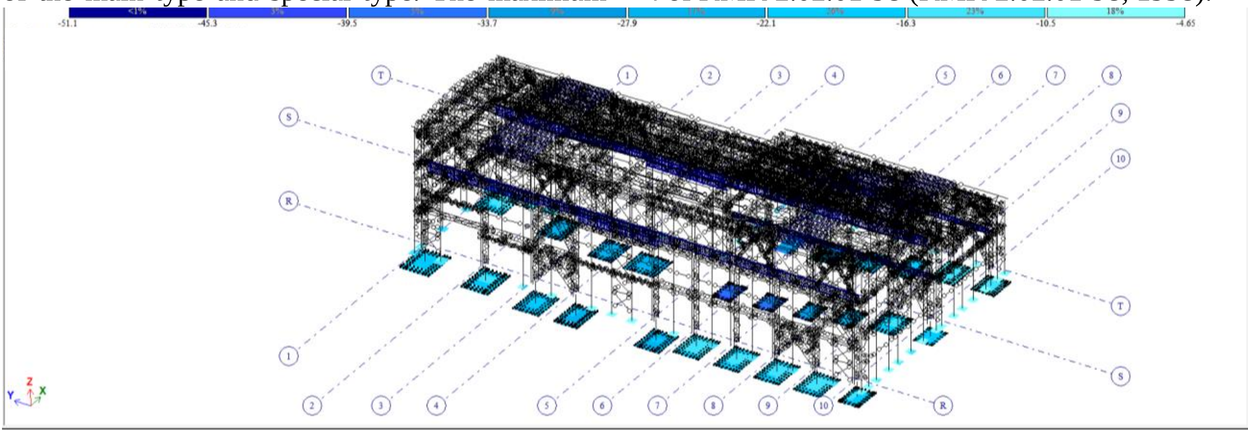

Figure 7. Vertical reaction from the soil mass

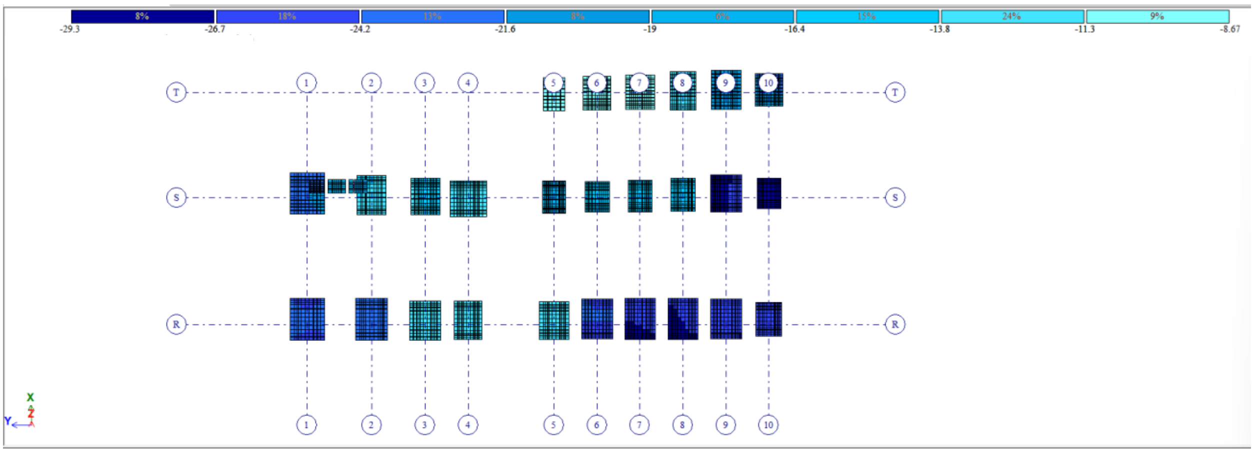

Figure 8. Vertical settlement of the foundation system

Originality and practical value

Thus, this publication provides an assessment of the effect of accounting for lateral soil pressure on the column footing of column monolithic reinforced concrete foundations. In particular, using the example of a foundation system for the steel frame of a two-span industrial building, the behavior of the foundation system was modeled using the LIRA-CAD software package, taking backfill into account. The soil bedding coefficient was adopted as the main modelling parameter. This assessment has been carried out for the first time, which constitutes its originality.

The practical significance lies in the quantitative adjustment of the reinforcement scheme for the foundation system and the determination of its load-bearing capacity. In doing so, account was taken not only of the influence of traditional static loads on industrial buildings of the type under consideration, but also of the influence of seismic loads characteristic of the site location – Bekabad in the Tashkent Region of Uzbekistan.

DOI: https://doi.org/10.15802/bttrp2026-29-02

Conclusions

1. Traditional approaches to the engineering design of shallow, isolated foundations for frame-type buildings do not take into account the lateral pressure exerted by the soil mass. In practical calculations, only the vertical pressure on the foundation bedding elements is considered.

2. The evaluation of the effect of lateral pressure from the soil mass has shown that this makes it possible to reduce the reinforcement of the column footing (by 1.5 … 2 times) and ensure more uniform performance of the entire building foundation system.

3. This practical approach can be recommended for the engineering design of similar building structures, as well as incorporated into the current regulatory framework of Ukraine.

REFERENCES

Alkhdour, A., Tiutkin, O., Bannikov, D., & Heletiuk, I. (2023). Substantiating the parameters for a non-circular structure of the mine shaft under construction in a heterogeneous rock massif. *IOP Conference Series: Earth and Environmental Science*, 1156, 012008. DOI: https://doi.org/10.1088/1755-1315/1156/1/012008

Bannikov, D. O., & Tiutkin, O. L. (2020). Prospective directions of the development of loose medium mechanics. *Science and Innovation*, 16(2), 42-50. DOI: https://doi.org/10.15407/scine16.02.045

Bofang, Z. (2018). *The finite element method: fundamentals and applications in civil, hydraulic, mechanical and aeronautical engineering*. Singapore: John Wiley & Sons Singapore Pte. Ltd. DOI: https://doi.org/10.1002/9781119107323

Chen, L. P., & Yang, Y. A. (2020). New Mixed Finite Element Method for Biot Consolidation Equations. *Advances in Applied Mathematics and Mechanics*. 6, 12, 1520-1541. DOI: https://doi.org/10.4208/aamm.OA-2019-0174

Dubinchyk, O., Bannikov, D., Kildieiev, V., & Kharchenko, V. (2020). Geotechnical analysis of optimal parameters for foundations interacting with loess area. *E3S Web of Conferences*, 168, 00024. DOI: https://doi.org/10.1051/e3sconf/202016800024

Petrenko, V., Bannikov, D., Kharchenko, V., & Tkach, T. (2022). Regularities of the deformed state of the geotechnical system «soil base – micropile». *IOP Conference Series: Earth and Environmental Science*, 970, 012028. DOI: https://doi.org/10.1088/1755-1315/970/1/012028

КМК 2.01.03-19. (2019). Сейсмик ҳудудларда қурилиш. Тошкент.

КМК 2.01.07-96. (1996). Юклар ва Таъсирлап. Тошкент.

КМК 2.02.01-98. (1998). Бино ва иншоотларнинг пойдеворлари. Тошкент.

Барабаш, М. С., Сорока, М. М., & Сур'янінов, М. Г. (2018). *Нелінійна будівельна механіка з ПК ЛІРА-САПР*. Одеса: Екологія.

ДБН В.2.1-10:2018 (2018). *Основи і фундаменти будівель і споруд. Основні положення*. Київ: Мінрегіон України.

ЛІРА-САПР. Приклади розрахунку і проектування. (2022). LIRALAND Group.

І. М. БАКАН

ТОВ «Сучасна будівельна компанія-груп», 3551 Сівард, кв. 342, Оушенсайд, Каліфорнія, США, 92056, тел. +38 (067) 436 91 21, ел. пошта sbc.group.ua@gmail.com, ORCID 0009-0008-4279-9793

ВРАХУВАННЯ БОКОВОГО ТИСКУ ҐРУНТУ ДЛЯ МОНОЛІТНИХ СТОВПЧАСТИХ ФУНДАМЕНТІВ ВИРОБНИЧИХ БУДІВЕЛЬ

Мета. Основною метою публікації є кількісна оцінка врахування бокового тиску ґрунтового масиву на характер армування фундаментної системи виробничої будівлі каркасного типу. **Методика.** Для досягнення поставленої мети була проаналізована робота моделі несучого каркасу двопрогонової виробничої будівлі ливарно-прокатного комплексу АО «Узметкомбінат» (місто Бекабад Ташкентської області Узбекистану). Габаритні розміри будівлі становлять 129×65,25 м при максимальній висоті 43,56 м. Фундаментна система прийнята роздільного типу із окремим фахверковим каркасом та виконана із монолітного залізобетону. Моделювання виконувалось засобами проєктно-обчислювального комплексу ЛІРА-САПР із додатковим модулем ГРУНТ. Моделювання виконувалось з урахуванням реальних ґрунтових умов. До уваги приймались не тільки традиційні статичні навантаження, але й сейсмічні впливи інтенсивністю в 8 балів. **Результати.** Проведене кількісне співставлення величин та характеру розподілу напружено-деформованого стану фундаментної системи показало, що врахування бокового тиску ґрунту зворотної засипки дозволяє зменшити потрібне армування на величину до 2-х разів. При цьому вдається отримати більш рівномірну картину роботи фу-

DOI: https://doi.org/10.15802/bttrp2026-29-02

ндаментної системи, що особливо важливо у випадках, коли окремі фундаменти мають різну глибину закладання. **Наукова новизна.** В ході проведеного аналізу визначено кількісно ступінь впливу бокового тиску від ґрунту зворотної засипки на фундаментну систему. Доведено необхідність її коректного моделювання, що суттєво впливає на характер напружено-деформованого стану фундаментної системи в цілому. **Практична значимість.** Отримані результати кількісної оцінки впливу бокового тиску на роботу монолітного фундаменту стовпчастого типу надають можливості не тільки більш обґрунтовано призначати схему армування фундаментної системи, а й відкривають перспективи для внесення такого підходу до нормативної бази України.

Ключові слова: фундаментна система; окремостоячий фундамент; сталевий каркас; коефіцієнт постелі; метод скінчених елементів; комплекс ЛІРА-САПР

REFERENCES

Alkhdour, A., Tiutkin, O., Bannikov, D., & Heletiuk, I. (2023). Substantiating the parameters for a non-circular structure of the mine shaft under construction in a heterogeneous rock massif. *IOP Conference Series: Earth and Environmental Science*, 1156, 012008. DOI: https://doi.org/10.1088/1755-1315/1156/1/012008 (in English)

Bannikov, D. O., & Tiutkin, O. L. (2020). Prospective directions of the development of loose medium mechanics. *Science and Innovation*, 16(2), 42-50. DOI: https://doi.org/10.15407/scine16.02.045 (in English)

Bofang, Z. (2018). *The finite element method: fundamentals and applications in civil, hydraulic, mechanical and aeronautical engineering*. Singapore: John Wiley & Sons Singapore Pte. Ltd. DOI: https://doi.org/10.1002/9781119107323 (in English)

Chen, L. P., & Yang, Y. A. (2020). New Mixed Finite Element Method for Biot Consolidation Equations. *Advances in Applied Mathematics and Mechanics*. 6, 12, 1520-1541. DOI: https://doi.org/10.4208/aamm.OA-2019-0174 (in English)

Dubinchyk, O., Bannikov, D., Kildieiev, V., & Kharchenko, V. (2020). Geotechnical analysis of optimal parameters for foundations interacting with loess area. *E3S Web of Conferences*, 168, 00024. DOI: https://doi.org/10.1051/e3sconf/202016800024 (in English)

Petrenko, V., Bannikov, D., Kharchenko, V., & Tkach, T. (2022). Regularities of the deformed state of the geotechnical system «soil base – micropile». *IOP Conference Series: Earth and Environmental Science*, 970, 012028. DOI: https://doi.org/10.1088/1755-1315/970/1/012028 (in English)

KMK 2.01.03-19. (2019). Seismyk ҳududlarda қurylysh. Toshkent. (in Uzbek)

KMK 2.01.07-96. (1996). Yuklar va Tasyrlap. Toshkent. (in Uzbek)

KMK 2.02.01-98. (1998). Byno va ynshootlarnynh poidevorlary. Toshkent. (in Uzbek)

Barabash, M. S., Soroka, M. M., & Surianinov, M. H. (2018). *Neliniina budivelna mekhanika z PK LIRA-SAPR*. Odesa: Ekolohiia. (in Ukrainian)

DBN V.2.1-10:2018 (2018). *Osnovy i fundamenty budivel i sporud. Osnovni polozhennia*. Kyiv: Minrehion Ukrainy. (in Ukrainian)

LIRA-SAPR. Pryklady rozrakhunku i proektuvannia. (2022). LIRALAND Group (in Ukrainian)

Article received: 26.01.2026.
Review date: 02.04.2026.
Publication date: 29.05.2026.